---

**Article:**
Kana Padinharu, D.K., Li, G.-J. orcid.org/0000-0002-5956-4033, Zhu, Z.Q. orcid.org/0000-0001-7175-3307 et al. (3 more authors) (2022) AC losses in form-wound coils of surface mounted permanent magnet Vernier machines. IEEE Transactions on Magnetics, 58 (6). 8105315. ISSN 0018-9464

https://doi.org/10.1109/TMAG.2022.3170658

---

# AC Losses in Form-Wound Coils of Surface Mounted Permanent Magnet Vernier Machines

D. K. Kana Padinharu[1], G. J. Li[1], *Senior Member, IEEE*, Z. Q. Zhu[1], *Fellow, IEEE*, R. Clark[2], A. Thomas[2], and Z. Azar[2]
[1]Department of Electronic and Electrical Engineering, The University of Sheffield, Sheffield, UK
[2]Siemens Gamesa Renewable Energy Limited, Broad Lane, Sheffield, UK
g.li@sheffield.ac.uk.

***Abstract*—Surface mounted permanent magnet Vernier (SPM-V) machines, because of their high torque density and multi-pole structure, are promising candidates for low speed direct-drive applications. To achieve high torque density, the SPM-V machines are generally designed with high gear ratios. Therefore, their operating frequencies can be much higher than those of the conventional SPM machines. This potentially increases the alternating current (AC) winding losses, especially those with form-wound coils proposed for high power applications. This paper investigates the AC losses (including skin effect, proximity effect, rotor PM induced and circulating current losses) in form-wound stator coils of a 3 MW direct-drive SPM-V machine with different slot/pole number combinations. The study reveals that the SPM-V machines have significantly higher AC winding losses than their conventional SPM counterparts for similar operating conditions. To reduce the AC winding losses in SPM-V machines, a novel flux shunt concept is proposed along with other conventional techniques such as increasing the number of turns/coil (with terminal voltage being kept constant) and parallel strands/turn, providing extra clearance at slot opening, etc. With the loss reduction techniques implemented, the SPM-V machines can achieve comparable efficiency but much higher torque density than their conventional counterparts. Moreover, the proposed flux shunt was also found to be very effective in reducing the potential risk of permanent magnet (PM) irreversible demagnetization, a key issue for SPM-V machines at high power ratings.**

**Keywords— AC loss, circulating current, efficiency, form-wound coil, Vernier machine.**

## I. Introduction

DIRECT-drive machines have recently gained popularity for wind power applications due to numerous advantages they offer over geared machines [1]. By eliminating the transmission system/gearboxes, direct-drive machines can achieve high reliability and overall system efficiency. However, high torque requirement at low speed may make them bulkier and heavier than their geared counterparts. It is widely recognized that permanent magnet (PM) machines are the most attractive candidates for direct-drive applications due to their high power density, efficiency and scalability [2]. Although the high cost of rare-earth PM materials has been a concern, these machines can still be competitive when long-term costs including operation & maintenance and design simplifications are considered [3].

In order to further improve the torque density and to reduce the PM material consumption, PM Vernier machines have emerged as a potential candidate [4]–[7]. One typical example is the surface mounted PM Vernier (SPM-V) machines, which have very similar structures to conventional surface mounted PM (SPM) machines. They work on the principle of flux modulation which enables them to have higher tangential airgap flux density to produce higher torque [8]. Moreover, they also produce inherently low torque ripple, which is desirable for direct-drive applications. However, the power factors of the SPM-V machines are often poor due to high leakage fluxes, which leads to increased power converter cost and also poor overall system efficiency [5], [9], [10]. In addition, to maximize the torque, the SPM-V machines are often designed with high number of rotor pole pairs and hence have higher operating frequency compared to conventional SPM machines [11], [12]. The high stator slot leakage fluxes combined with the high operating frequency of SPM-V machines can result in elevated level of stator winding alternating current (AC) losses. Moreover, the SPM-V machines often require an open stator slot structure to utilize the flux modulation effect, leading to increased fringing fluxes generated by rotor PMs and armature currents. This, together with the form-wound windings used for multi-MW machines, can increase the AC winding losses to an even higher level.

Earlier studies have shown that the efficiency of Vernier machines for direct-drive wind application can be comparable to that of conventional machines [4], [5], [13]. However, the electromagnetic losses used for the efficiency calculation did not include the AC winding losses. Irrespective of the applications, the AC winding losses in Vernier machines have rarely (if not at all) been investigated in literature. It is very important to analyze these losses to benchmark the efficiency and thermal performance of SPM-V machines in comparison with the conventional SPM machines.

The AC winding losses are generated when time varying magnetic fields link with a conductor and the different sources of AC winding losses can be classified as [14]–[16]:

(1) Skin effect: Losses due to non-uniform distribution of current density within a conductor created by the high frequency time-varying current carried by it. The distribution of the current density within the conductor is characterized by the skin depth defined as the distance from the outer periphery of the conductor at which the current density is ~0.3678 of the value on the surface [17]. Skin depth ($\delta$) is a function of the electrical properties of the conductor and the operating frequency ($f$) of the current, described by

$$\delta = \sqrt{\frac{\rho}{\pi f \mu_o \mu_r}} \quad (1)$$

where $\rho$ and $\mu_r$ are the resistivity and the relative permeability of the conductor, respectively. $\mu_o$ is the free space permeability ($4\pi \times 10^7$ H/m).

(2) Proximity effect**:** Losses created in a conductor due to currents carried by adjacent conductors. Earlier studies reveal that proximity effect is largely contributed by the slot leakage fluxes in PM machines [14], [17], [18]. The AC losses due to both 'skin effect' and 'proximity effect' have been extensively studied for different PM machine topologies with varying slot geometries, winding configurations, conductor shapes and current signals [14], [15], [17]–[22]. Most of these studies have been carried out for high speed (~10000-20000 rpm) applications where the AC resistance of the conductor

increases with operational speed/frequency due to skin effect and proximity effect. These losses can also be driven by high frequency harmonics in pulse width modulated (PWM) signals [20], [23]. However, for simplicity, only the fundamental component of power source will be considered in this paper.

(3) Rotor PM induced [14]: Losses in PM machines due to the rotating PM fluxes linking with the stationary conductors. These losses can be significant for open slot PM machines [14], [15], [17] due to significant fringing fluxes near stator tooth tips.

(4) Circulating current: Losses due to circulating currents in windings with multiple parallel strands per turn. Generally, the parallel strands of each turn are short-circuited or brazed at the end of each coil. When a time-varying magnetic field links with this short-circuited path, a circulating current is generated [17]. These losses can be significant for high-speed applications where multiple parallel strands are used as a solution to mitigate the losses due to skin and proximity effect [16], [17].

This paper presents a systematic study of AC winding losses in a 3 MW direct-drive SPM-V machine with form-wound coils. The study considers all sources of AC winding losses such as skin effect, proximity effect, rotor PM induced and circulating current. The losses have been compared with those of a conventional SPM machine with similar operating conditions. Different slot/pole number combinations have been considered for the SPM-V machines to achieve optimal efficiency. Additionally, the paper also presents various solutions through analysis to mitigate the high AC winding losses in the SPM-V machines.

## II. Basic Features of Vernier Machines

The one pole pair 2D finite element analysis (FEA) models for the 3 MW conventional SPM and SPM-V machines are shown in Fig. 1. For Vernier machines to utilize the flux modulation/gearing effect, the slot/pole number combination follows the rule [11], [12]

$$P_r = N_s \pm P_s \tag{2}$$

where $N_s$ is the number of stator slots, $P_r$ is the rotor pole pair number and $P_s$ is the stator winding pole pair number.

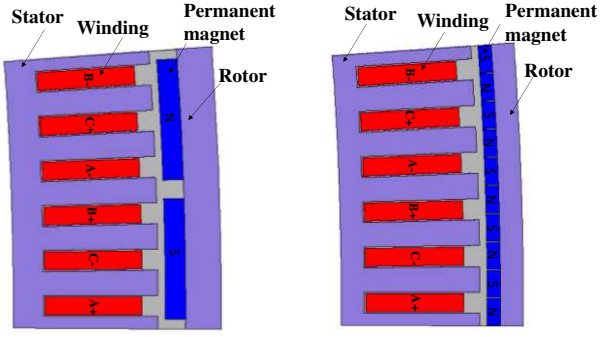


(a) (b)

Fig. 1 One pole pair 2D FEA models. (a) Conventional SPM machine with $N_s = 480, P_r = 80, P_s = 80$, and (b) SPM-V machine with $N_s = 480, P_r = 400, P_s = 80$.

In a Vernier machine, its fundamental ($P_s$th order) armature Magneto-Motive Force (MMF) interacts with the fundamental component of the airgap permeance ($N_s$th order, created by open stator slots) to produce a modulated airgap flux density component of $(N_s \pm P_s)^{\text{th}}$ order. In addition, the $(N_s \pm P_s)^{\text{th}}$ order is also a slot harmonic component of the armature field. Unlike the conventional SPM machines, the rotor pole pair number ($P_r$) for the SPM-V machines is selected such that it matches with the modulated/slot harmonic order (2). Therefore, in the example shown in Fig. 1, $P_r$ for the SPM-V machine is 400, which matches with the difference between the slot number ($N_s = 480$) and the stator winding pole pair number ($P_s = 80$). It is observed that by harmonically coupling the fields in the SPM-V machines, a significantly higher tangential airgap flux density can be produced compared to the conventional SPM machines [8]. This enables the SPM-V machines to produce higher torque. The ratio of the harmonic order of the modulated flux density to that of the fundamental armature flux density is defined as the gear ratio ($G_r$) of the SPM-V machines. Therefore, the gear ratio is given by

$$G_r = \frac{N_s \pm P_s}{P_s} = \frac{P_r}{P_s} \tag{3}$$

SPM-V machines are generally designed with higher gear ratios to achieve higher torque [11]. However, a higher gear ratio would mean a high number of rotor pole pairs and thereby increased PM leakage flux. Therefore, for SPM-V machines, higher torque is often achieved at the cost of poor power factor.

The operating frequency ($f$) of the SPM-V machines is given by

$$f = P_r \omega_r / 2\pi \tag{4}$$

where $\omega_r$ is the rotor mechanical speed in rpm. It is worth noting that for a similar stator structure as shown in Fig. 1 and the same rotor speed, the operating frequency of the SPM-V machines will be $G_r$ times higher than that of the conventional SPM machine. This can potentially increase the winding AC losses in the SPM-V machines. Similarly, unlike the conventional SPM machines, the SPM-V machines also require an open stator slot structure to utilize the modulation effect, irrespective of the type of winding (form or random wound). The open stator slots increase the fringing fluxes linking with the stator winding and thereby increase the AC winding losses. Therefore, it is important to analyze the AC winding losses for SPM-V machines with different slot/pole number combinations. This helps to identify the optimal slot/pole number combination for the SPM-V machine topology for the direct-drive wind application.

## III. Modelling and Validation of AC Losses

### A. Slot/Pole Number Combinations

A 3 MW direct-drive conventional SPM machine with an outer rotor as shown in Fig. 1(a) is chosen for benchmarking the performance of SPM-V machines. The magnetic periodicity of the SPM-V machine is equal to the modulated field or stator winding pole pairs ($P_s$), which requires a 6 slot model for a 3-phase machine similar to the conventional SPM machine.

TABLE I. Key Parameters for Conventional SPM Machine

| | | | |
|---|---|---|---|
| Rated Power (MW) | 3.0 | Stack length (mm) | 1200 |
| L-L voltage (Vrms) | 690 | Magnet material | NdFeB |
| Phase current (Arms) | 2694 | Magnet volume ($m^3$) | 0.227 |
| Rotor speed (rpm) | 15 | Magnet remanence (T) | 1.3 |
| Rotor outer diameter (mm) | 5000 | Copper conductivity (S/m) | $5.77e^7$ |
| Air gap length (mm) | 5 | Slot fill factor | 0.6 |

OPERA software package has been used for the finite element modeling and analysis presented in this paper. The key parameters of the conventional SPM machine are listed in TABLE I. An outer rotor topology is selected as it is more favorable for direct-drive applications [24]. To accommodate form-wound coils, the stator is designed with open slots. The machine has integer slot windings with slots/pole/phase equal to 1. For a fair comparison, the SPM-V machines are designed with the same rotor outer diameter, magnet volume and DC copper loss (for the active length). It is also worth noting that, for the analyses in this paper, all the machines are globally optimized for maximum torque using the OPERA optimizer tool [uses a combination of deterministic (sequential quadratic programming) and stochastic method (genetic algorithms, simulated annealing)]. The previous studies have found that the power factors of MW direct-drive SPM-V machines designed with a gear ratio equal to 5 are quite low (~0.4-0.5) [25]. Selecting a higher gear ratio will further lower the power factor. Hence, a gear ratio of 5 has been chosen for this study which is also the minimal number to realize an integer slot winding for the SPM-V machines. For this gear ratio, different slot/pole number combinations are possible as long as they satisfy (2). Some possible slot/pole number combinations chosen for this study are given in TABLE II. The operating frequencies of these machines as highlighted in TABLE II are proportional to the rotor pole pair numbers. It can be observed that, with similar stator structures, the frequencies of the SPM-V machines are 5 times higher than those of the conventional SPM machines. Due to the poor power factor, the SPM-V machines generate much higher terminal voltage than the conventional SPM machines for the same number of turns/phase. Hence to maintain the same terminal voltage (690 V), the number of turns/phase for the SPM-V machines (as shown in TABLE II) needs to be much lower than that of the conventional SPM machines.

### *B. Modelling of Stator Winding AC losses*

The stator windings, as mentioned before, are designed with form-wound coils, generally used for high power applications as they are necessary to increase the slot fill factor and simplify the winding process. In addition, rectangular conductors not circular conductors have been used as the former generally achieves higher slot fill factor. The stator slot layout used for this study is shown in Fig. 2. Having the same terminal voltage allows using the same ground wall insulation thickness, assumed as 1 mm, for both the conventional SPM and SPM-V machines. The number of parallel circuits in each phase is adjusted so that the numbers of turns/coil for both the SPM-V and the conventional SPM machines are as close as possible (see TABLE II). Each turn of the coil is assumed to have two parallel strands. The numbering of the strands in the slot is shown in Fig. 2 with strand number 1 being located nearest to the airgap. To consider the skin effect in the strands, dense mesh with at least 4 layers of elements is placed in the skin depth. The turn insulation is neglected for simplifying the model. However, assigning separate conductor numbers to each strand in OPERA software allows the eddy currents to be confined within the strands.

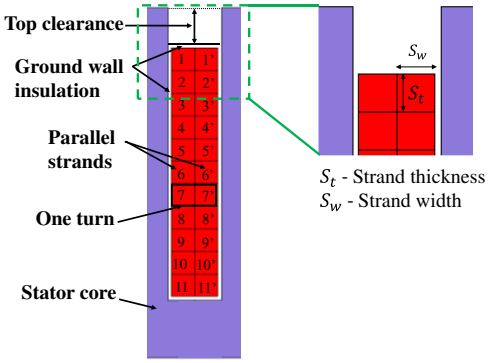


Fig. 2 Example of slot layout of the investigated machine.

A 10 mm clearance is provided at the top of the slot near the airgap to accommodate slot wedges. The conductivity of copper is assumed to be 5.77e$^7$ S/m (at 20°C) and any temperature dependence is not considered in this study for simplicity. However, it is worth noting that with higher temperature, the copper resistance will increase and associated effects on the DC and AC losses might need to be considered. Similarly, the AC winding losses due to end effects such as end-winding flux, axial flux from PMs, etc. have not been considered in this study. However, end winding resistance and inductance [26] have been considered for the DC and circulating current losses (connected as an external circuit).

An example of the circuit schematic of one coil (with 2 parallel strands and 11 turns/coil) for estimating the circulating current is shown in Fig. 3. The parallel strands are assumed to be short-circuited/brazed at the end of each coil. For this study, no transposition of strands is employed.

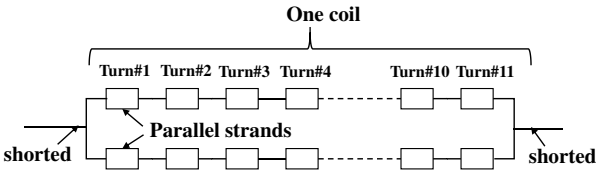


Fig. 3 An example of the circuit schematic of one coil with 2 parallel strands and 11 turns/coil. The parallel strands of each coil are short-circuited at the end of the coil.

### *C. Validation of FE Modelling*

The modelling approach used in this paper is validated by comparing the AC winding losses against those presented in [27], wherein the open-circuit AC winding losses in a 12-slot/8-pole SPM machine with inner rotor have been calculated by both 2D FE and analytical models. The comparison of the 2D FE models along with the open-circuit flux distributions are shown in Fig. 4. The open-circuit AC winding losses for a winding configuration with 4 radial and 4 circumferential layers (as shown in Fig. 4) for different

TABLE II. DETAILS OF SLOT/POLE NUMBER COMBINATIONS AND STATOR WINDING CIRCUIT

| Machine Type | Stator slot number ($N_s$) | Rotor pole pair ($P_r$) | Stator winding pole pair ($P_s$) | Operating frequency (Hz) | Turns/phase | Turns/coil | Number of parallel circuits |
|---|---|---|---|---|---|---|---|
| Conventional | 480 | 80 | 80 | 20 | 56 | 14 | 20 |
| Vernier | 192 | 160 | 32 | 40 | 22 | 11 | 16 |
| Vernier | 240 | 200 | 40 | 50 | 22 | 11 | 20 |
| Vernier | 360 | 300 | 60 | 75 | 22 | 11 | 30 |
| Vernier | 480 | 400 | 80 | 100 | 22 | 11 | 40 |

speeds are compared in Fig. 5. The AC winding losses calculated using the 2D FE modelling in this paper are found to be in very good agreement with those obtained in [27].

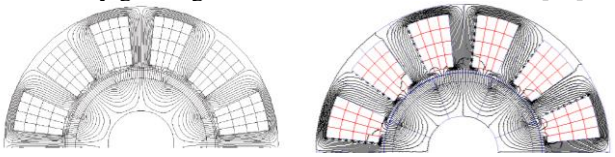

(a) (b)

Fig. 4 Comparison of open-circuit flux distribution of a 12slot/8pole SPM machine predicted by (a) 2D FE modelling in [27] (b) 2D FE modelling used in this paper.

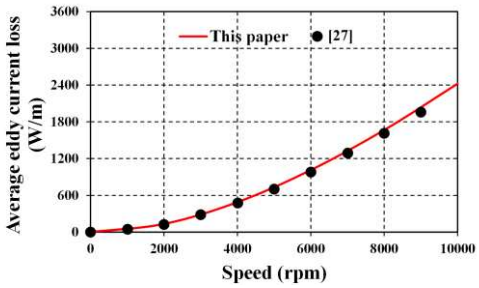


Fig. 5 Comparison of FE results for open-circuit AC winding losses with increasing machine speed for a 12-slot/8-pole SPM machine [27] with each coil having 4 radial and 4 circumferential layers.

## IV. 2D FE Results for AC Winding Losses

The calculated skin depth using (1) for the designs mentioned in TABLE II along with their strand thicknesses and widths are shown in TABLE III. It can be observed that the skin depth is comparable to the strand dimensions and hence the losses associated with 'skin effect' will be negligible for this study.

TABLE III. Skin Depth For Winding Strands

| Machine Type | Rotor pole pair ($P_r$) | Strand thickness, $S_t$ (mm) | Strand width, $S_W$ (mm) | Skin depth, $\delta$ (mm) |
|---|---|---|---|---|
| Conventional | 80 | 4.82 | 6.3 | 14.8 |
| Vernier | 160 | 5.0 | 20 | 10.5 |
| Vernier | 200 | 5.45 | 15 | 9.4 |
| Vernier | 300 | 5.45 | 8.63 | 7.7 |
| Vernier | 400 | 5.95 | 6.27 | 6.6 |

The 2D FE non-linear transient analysis has been performed for three different operating conditions:

- 'Open-circuit' analysis with only PM excitation. In this analysis, AC winding losses are mainly due to 'rotor PM induced' and 'circulating current' components.
- 'Armature only' analysis with only armature excitation. In this analysis, the winding loss will have components of 'proximity effect' losses, DC losses (due to rated current) and circulating current losses.
- 'Rated load' analysis with both PM and armature current excited. In this analysis, all the loss components will contribute to the AC winding losses.

Other losses like PM eddy current losses, stator and rotor core losses are also included for rated load case to estimate the efficiency of the machines. Since the SPM-V machines are found to have high PM eddy loss, each PM is segmented with 4 circumferential segments to reduce the PM eddy current loss for this study.

### A. Open-Circuit Analysis

The comparison of winding losses under open-circuit condition between the conventional SPM and SPM-V machines is shown in Fig. 6. The losses presented are for the entire machines. The winding losses for the SPM-V machines become significantly higher (maximum is 99 kW) towards lower slot/pole numbers compared to the conventional SPM machine (0.3 kW). The winding loss is mainly contributed by the 'Rotor PM induced' component. Whereas the 'circulating current' loss component is negligible. However, both loss components show an increasing trend towards lower slot/pole numbers. This is due to the large slot opening at low slot/pole numbers and thereby higher PM fringing fluxes linking with the windings.

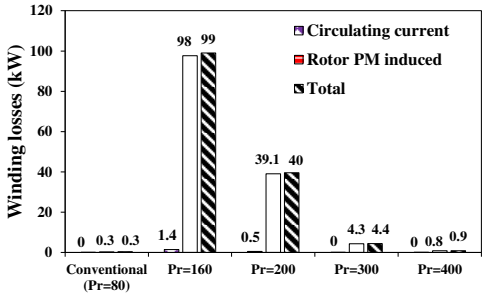


Fig. 6 Comparison of winding losses under open-circuit condition between the conventional SPM and SPM-V machines with different slot/pole number combinations. $N_s$ for the corresponding $P_r$ are given in TABLE II.

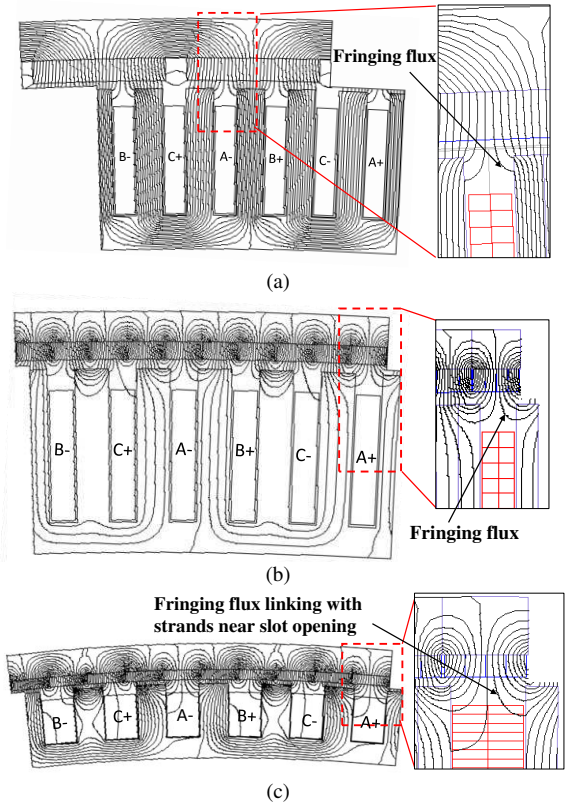


Fig. 7 Comparison of open-circuit flux distributions. (a) Conventional SPM machine, (b) SPM-V machine with $P_r = 400$ and (c) SPM-V machine with $P_r = 160$. The rotor position is selected such that the phase A winding has maximum flux linkage.

The open-circuit flux distributions of the highest and the lowest slot/pole number combination of SPM-V machines in comparison with the conventional SPM machine are shown in Fig. 7. It can be observed that at low slot/pole numbers, there is more PM leakage/fringing flux linking with the top conductors nearest to the airgap resulting in higher AC winding losses.

The comparison of current density distributions within one coil side of phase A (at the position where the winding loss is maximum) between the conventional SPM and two SPM-V

machines ($P_r = 400$ and $P_r = 160$) is shown in Fig. 8. The current density is contributed by the rotor PM induced and circulating currents. It can be observed that the current density is highly concentrated at the first few turns of the coil nearest to the airgap with a maximum value of 27.14 A/mm$^2$ for $P_r = 160$. The average loss in each strand per turn in a slot is shown in Fig. 9. Again, the trend shows a high loss concentration in strands near the airgap (or slot opening).

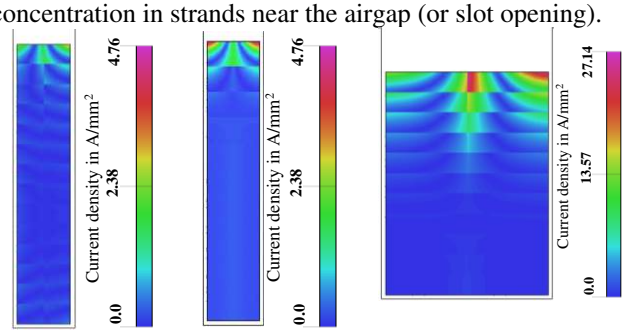


(a) (b) (c)

Fig. 8 Current density distributions within one coil side of phase A (at maximum winding loss position). (a) Conventional SPM machine. (b) SPM-V machine with $P_r = 400$. (c) SPM-V machine with $P_r = 160$.

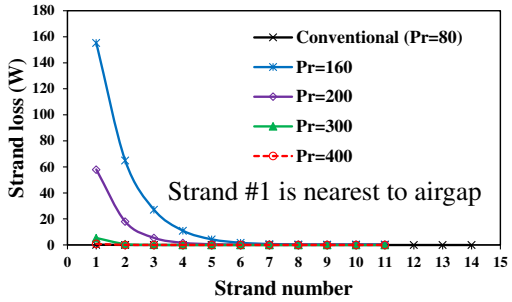


Fig. 9 Trend of open-circuit average losses in each strand per turn in a slot. Strand 1 is nearest to the airgap.

To explain the above observations, the eddy-current loss per unit volume in a solid conductor can be used, which can be calculated by [28]

$$P_v = \frac{\pi^2 f^2 {B_m}^2 w^2}{6\rho} \tag{5}$$

where $B_m$ is the maximum instantaneous flux density impinging on the conductor, $f$ is the frequency, $w$ and $\rho$ are the width (perpendicular to the direction of $B_m$) and resistivity of the conductor, respectively.

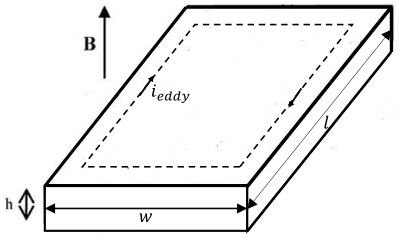


Fig. 10 Schematic of a solid conductor (length-$l$, width-$w$, thickness-$h$) carrying eddy current, $i_{eddy}$, due to a magnetic flux density $B$ impinging perpendicular to the width.

It can be observed from (5) that besides the flux linking with the conductors, the AC winding losses are also $\propto f^2 w^2$. $f$ of the SPM-V machines as shown in TABLE II are higher than the conventional SPM machines, especially towards higher slot/pole numbers. Moreover, it can be observed from TABLE III that $w$ significantly increases towards the lower slot/pole number. The high PM fringing flux along with 2 times higher $f$ and 3 times wider $w$ makes the winding loss significantly higher in the SPM-V machines at the lowest slot/pole number compared to the conventional SPM machines.

### *B. Armature Only Analysis*

The comparison of winding losses between the conventional SPM machines and SPM-V machines with only 3-phase sinewave armature currents excited are shown in Fig. 11. It is to be noted that as this is a current-fed model, the same rated current is forced in the circuit despite any increase in AC resistance. The 'circulating current' and the DC loss contributions can be calculated from the known currents and resistance values. 'Proximity effect' loss component can then be segregated from the total predicted loss. The SPM-V machines again show significantly higher winding losses with a maximum of 361.9 kW at the highest slot/pole number ($P_r = 400$) compared to the conventional SPM machine (54.5 kW). Contrary to the trend of 'rotor PM induced' losses under open-circuit condition, the 'proximity effect' loss component shows an increasing trend towards higher slot/pole numbers for the SPM-V machines. The DC loss including end winding loss is almost constant for all the machines (ranging from 46 kW to 49 kW). The 'circulating current' loss component is found to be negligible with a maximum value of 0.3 kW for the SPM-V machines with the lowest slot/pole number ($P_r = 160$).

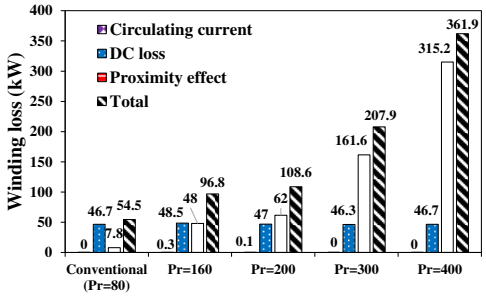


Fig. 11 Comparison of winding losses with only armature current excited between the conventional SPM and SPM-V machines with different slot/pole number combinations.

The flux distributions with only armature currents excited for the conventional SPM machines and the SPM-V machines with $P_r = 400$ and $P_r = 160$ are shown in Fig. 12. It can be observed that at high slot/pole number, the slot leakage flux is very dominant as highlighted in Fig. 12(a) and (b). This is due to the relatively larger magnetic airgap length compared to the slot width. Although the conventional SPM machine also has high slot leakage fluxes due to similar stator structure, its operating frequency will only be 1/5$^{th}$ that of the SPM-V machines.

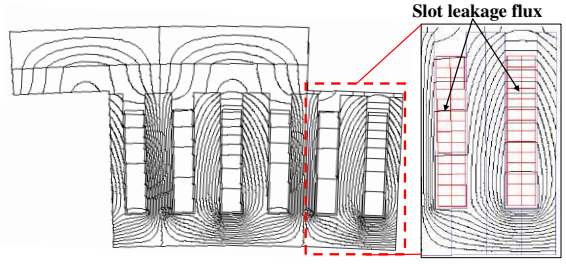


(a)

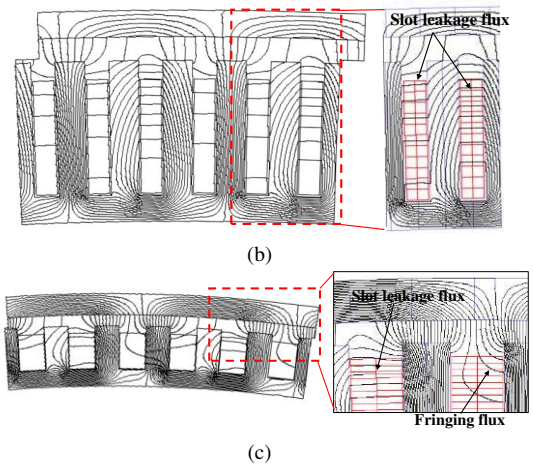


Fig. 12 Comparison of flux distributions with only armature currents excited. (a) Conventional SPM machine. (b) SPM-V machine with $P_r = 400$. (c) SPM-V machine with $P_r = 160$.

To verify the significantly high AC winding loss in the SPM-V machine with $P_r = 400$, the losses are approximately calculated using (5). The losses of the conventional SPM machine are used as reference. Some assumptions are made here to simplify the analyses, i.e. the dominant source of loss is the stator slot leakage flux and the flux magnitude is approximately the same for these two machines. These assumptions are deemed as acceptable as both machines have a very similar stator structure. Also, the direction of slot leakage fluxes is assumed to be perpendicular to the slot wall. Therefore, the AC winding loss ($P_{ver(P_r=400)}$) in the SPM-V machine with $P_r = 400$ is given by

$$\begin{aligned} P_{ver(P_r=400)} &= P_{con} \times \left(\frac{f_{ver}}{f_{con}}\right)^2 \left(\frac{w_{ver}}{w_{con}}\right)^2 \\ &= 7.8 \times \left(\frac{100}{20}\right)^2 \left(\frac{5.95}{4.82}\right)^2 \\ &= 297.15\ kW \end{aligned} \tag{6}$$

where $P_{con}$ is the AC winding loss of the conventional SPM machine, $f_{ver}$ and $f_{con}$ are the operating frequencies (as highlighted in TABLE II) of the SPM-V machine (with $P_r = 400$) and conventional SPM machine, respectively. $w_{ver}$ and $w_{con}$ are the strand thicknesses (as highlighted in TABLE III) of the SPM-V machine (with $P_r = 400$) and the conventional SPM machine, respectively. The calculated loss is close to that predicted by 2D FEA (315.2 kW). This gives more confidence in the adopted methodology and also supports the reasoning behind high AC winding losses in SPM-V machines with high slot/pole numbers.

For the SPM-V machines with low slot/pole number combinations, the slot leakage flux is negligible due to their large slot opening. However, they have a high fringing flux component that links with the top conductors (near to airgap) compared to the SPM-V machines with high slot/pole number combinations, as shown in Fig. 12(c). The average strand losses (excluding DC loss) at different strand numbers (with strand number 1 nearest to the airgap) in a slot are shown in Fig. 13. Similar to open-circuit losses, the trend of strand losses with only armature currents excited also shows a high concentration of losses in the top conductors near the airgap. The strand losses at high slot/pole numbers show a rather constant decreasing trend towards the slot bottom. This is because, the slot leakage fluxes, which is the main source of winding losses at high slot/pole numbers, also have a uniformly decreasing magnitude towards the slot bottom. However, for low slot/pole numbers, the losses are mainly driven by the fringing fluxes which are concentrated in the strands near the airgap. Hence, a sharper decrease of losses is observed in the first few turns. After that, the decrease tends to slow down. Unlike the open-circuit losses, the armature only losses penetrate further down to the conductors near the slot bottom.

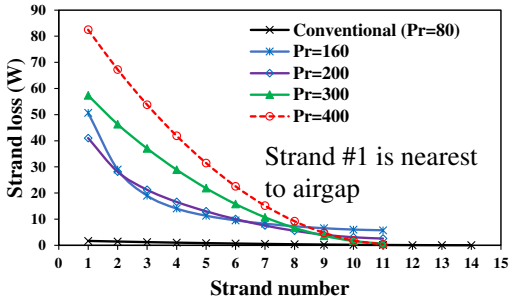


Fig. 13 Trends of average strand losses in a slot with only armature currents excited. Strand 1 is nearest to the airgap.

## C. Rated Load Analysis

The rated load analysis combines the effects of PM and armature fields. The comparison of winding losses between the conventional SPM and SPM-V machines under rated load is shown in Fig. 14. The losses are found to be almost equal to the summation of the losses under open-circuit and armature only analyses. The maximum winding loss, around 362.6 kW, is in the SPM-V machines with $P_r = 400$. This loss is significantly higher compared to the total winding loss (55.5 kW) in the conventional SPM machine. The minimum winding loss (148.8 kW) is achieved by the SPM-V machines with $P_r = 200$. However, it is still almost 3 times that of the conventional SPM machine.

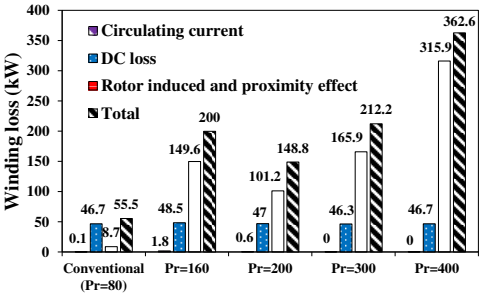


Fig. 14 Comparison of winding losses under rated load condition between the conventional SPM and SPM-V machines with different slot/pole number combinations.

The average torques for the SPM-V machines with different slot/pole numbers are compared against the conventional SPM machines, as shown in Fig. 15. The average torque is found to be increasing towards lower slot/pole numbers. With lower winding losses and higher average torque, the lower slot/pole numbers would be better choices for the SPM-V machines.

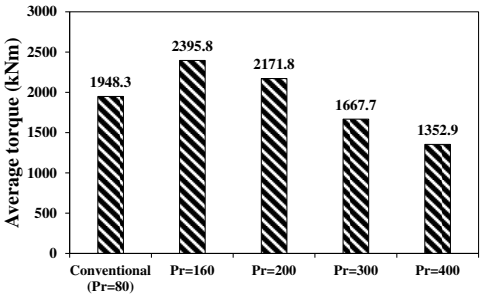


Fig. 15 Comparison of average torques between the conventional SPM and SPM-V machines with different slot/pole number combinations.

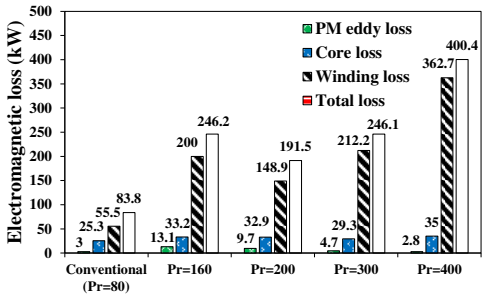


Fig. 16 Comparison of electromagnetic losses at rated load between the conventional SPM and SPM-V machines with different slot/pole number combinations.

The electromagnetic losses required to evaluate the machine efficiency are compared in Fig. 16. This shows that the winding losses (DC+AC) are significantly higher than other electromagnetic losses for the SPM-V machines and therefore cannot be neglected. It is interesting to note that although the operating frequencies of the SPM-V machines are higher, the core loss is not proportionally higher (~1.3 times) than that of the conventional SPM machines. This is because, due to high inter-pole leakage fluxes, less PM fluxes penetrate into the stator core. The efficiency of the machines with and without considering the AC winding losses is shown in Fig. 17. Without considering the AC winding losses, the highest efficiency achieved by the SPM-V machines with $P_r = 160$ can be comparable to the conventional SPM machine. However, the AC winding losses have markedly reduced the efficiency of the SPM-V machines, especially at high slot/pole number. The highest efficiency (94.7%) is achieved by the SPM-V machine with $P_r = 200$.

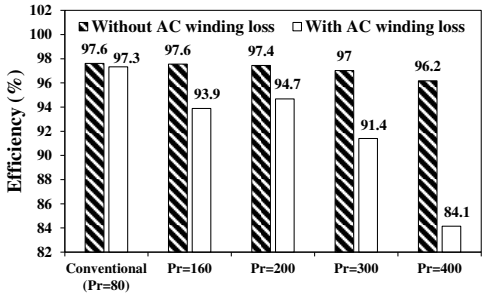


Fig. 17 Comparison of efficiencies with and without considering the AC winding losses at rated load between the conventional SPM and SPM-V machines with different slot/pole number combinations.

The efficiency of the SPM-V machines is significantly reduced due to the AC winding losses and hence requires loss reduction techniques to be competitive against the conventional SPM machines. Some of the existing techniques like increasing the number of turns and strands [17], [18], [21], placing the conductors away from slot opening [16], [22], etc. are investigated in this paper. Section V discusses in detail the effectiveness of these techniques in reducing the AC winding losses in the SPM-V machines.

## V. Effect of Conventional AC Winding Loss Reduction Techniques

This section investigates the effect of the following parameters on the winding loss of the SPM-V machines:

- **Turns/coil:** The number of turns/coil effectively changes the strand thickness and thereby influences the winding losses caused by the fluxes such as slot leakage fluxes which are mostly perpendicular to slot wall.
- **Parallel strands/turn:** The number of strands/turn changes the strand width and therefore can influence the winding losses caused by the fluxes like fringing fluxes penetrating in the radial direction.
- **Extra clearance near slot opening:** Providing extra clearance at the slot opening can protect the first few strands, which experience maximum losses due to fringing fluxes. Since the slot depth is not changed, the conductors become thinner and this further reduces the AC winding losses. However, the DC winding losses will increase with the reduced conductor cross-sectional area.

### A. *Effects of Number of Turns/Coil*

To demonstrate the effectiveness of number of turns/coil in reducing the AC winding loss, the slot leakage flux and the resultant eddy current directions are shown in Fig. 18. The slot leakage fluxes in X-axis create eddy current in Y-Z plane as highlighted by the yellow contours. To reduce the magnitude of this eddy current, the coil should be segmented either in Y or Z-axis. Segmenting the coil in Z-axis or along the axial length of the machine is impossible as a continuous conductor is required. Segmenting in Y-axis effectively points towards increasing the number of turns/coil. Therefore, increasing the number of turns/coil can be effective to reduce the AC winding losses created by the X-axis fluxes like slot leakage fluxes.

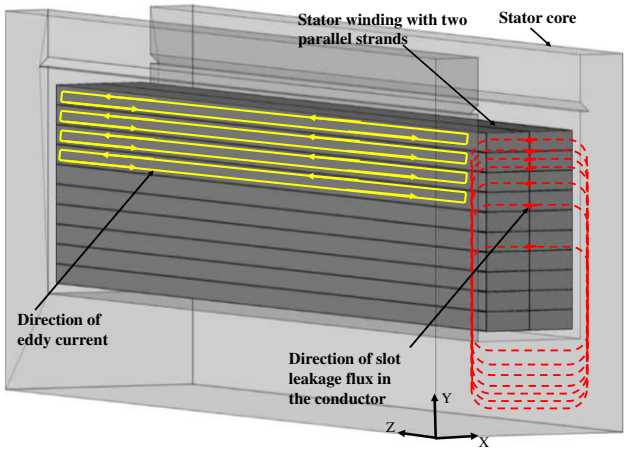


Fig. 18 Direction of eddy current in strands due to slot leakage fluxes created by armature current only.

For this sensitivity analysis, the number of turns/coil is firstly increased from 11 to 22 without changing the series turns/phase to maintain the same terminal voltage level. This is achieved by doubling the parallel circuits (in TABLE II) of every SPM-V machine. Thereafter, the number of turns/coil is progressively reduced to a minimum value of 11. While doing this, the strand thickness progressively increases and accordingly the current carried by the strands increases to maintain the same DC copper loss and average torque. Although the terminal voltage reduces (not a desirable choice) proportionally to the turns/coil, these results can be useful for the parameter sensitivity analysis. It is worth noting that the slot fill factor has been kept constant while changing the number of turns/coil.

With only armature currents excited, the trends of AC winding losses (excluding circulating current and DC winding losses) with increasing number of turns/coil for the SPM-V machines with different slot/pole number combinations are shown in Fig. 19. The AC winding losses are represented as a normalized value. 11 turns/coil is taken

as reference for each slot/pole number combination. It can be observed that for high slot/pole numbers, increasing the number of turns/coil is very effective in reducing the AC winding losses. This is because the main source of winding losses is slot leakage fluxes which are mostly perpendicular to slot wall. Increasing the turns/coil from 11 to 22 could reduce the AC winding loss by 75% for both $P_r = 400$ and $P_r = 300$. If the slot leakage flux was the sole reason for the AC winding losses, the normalized loss curves would all overlap each other like $P_r = 400$ and $P_r = 300$. However, due to the dominant fringing flux towards lower slot/pole number, the normalized curve deviates from the expected trend. Since the fringing fluxes change from circumferential direction to radial direction, the effectiveness of increasing turns/coil to reduce the AC winding losses diminishes (to 41%) for low slot/pole numbers.

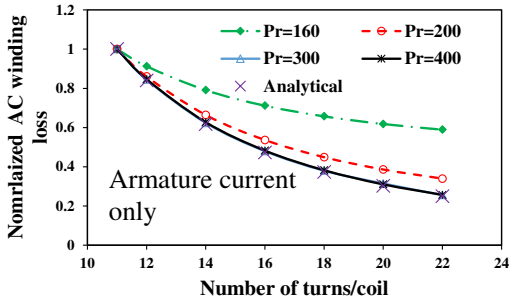


Fig. 19 Trends of AC winding losses with increasing number of turns/coil for different slot/pole numbers of the SPM-V machines with only armature currents excited.

The trend of normalized AC winding loss with turns/coil can also be analytically calculated using (5) assuming the value to be equal to 1 at 11 turns/coil. The losses will be proportional to the square of the strand thickness assuming the flux to be perpendicular to slot wall. It is observed that the analytically calculated values perfectly match with the normalized curves of the SPM-V machines with $P_r = 400$ and $P_r = 300$, as shown in Fig. 19.

The circulating current loss was found to be unaffected by the number of turns/coil. Since the copper loss is maintained the same for different numbers of turns/coil, the DC loss also remains unchanged for a given slot/pole number.

The trends of open-circuit AC winding losses with turns/coil for SPM-V machines with different slot/pole number combinations are shown in Fig. 20. It can be observed that at low slot/pole numbers, where the open-circuit AC winding losses are significant, increasing the turns/coil is not effective. However, at high slot/pole numbers, it is found to be effective (it can reduce AC winding loss by 24%) but the loss magnitudes themselves are very much negligible. Therefore, in general, it can be concluded that increasing the number of turns/coil is an effective way to reduce the AC winding losses due to the slot leakage fluxes.

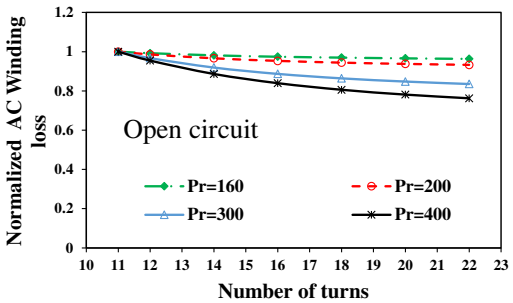


Fig. 20 Trends of open-circuit AC winding losses with increasing number of turns/coil for SPM-V machines with different slot/pole numbers.

## B. *Effects of Number of Parallel Strands/Turn*

The induced eddy current distribution in the strands due to magnetic fluxes in Y-axis is shown in Fig. 21.

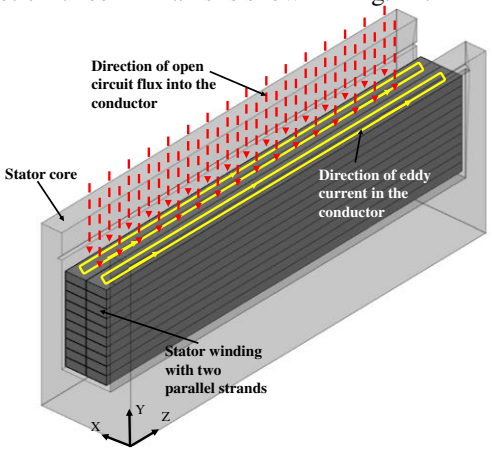


Fig. 21 Schematic showing the distribution of induced eddy currents in the strands due to Y-axis fluxes.

The magnitude of eddy currents generated in X-Z plane can be reduced by segmenting the conductors either in X or Z-axis. The possible direction of segmentation is in X-axis which is equivalent to having more parallel strands/turn. Therefore, having more parallel strands/turn can be effective in reducing the winding losses generated by fluxes in Y-axis (or in radial direction). This means that they can be effective in reducing the losses towards lower slot/pole numbers which have more fringing flux components.

The number of parallel strands/turn is increased from 1 (single strand) to 4 in the baseline design (TABLE II) to investigate their effect on the winding losses. No transposition of parallel strands has been considered in this analysis. Hence, all the parallel strands of a turn are in the same vertical position with respect to the slot depth. The variation of open-circuit AC winding loss (excluding circulating current loss) against increasing number of parallel strands/turn is shown in Fig. 22(a). The AC winding losses are represented as a normalized value with the losses of 1 strand/turn taken as reference for each slot/pole number. It can be observed that a sharp decrease of AC winding losses (55-67%) happens when the parallel strands are increased from 1 to 2. Beyond 2, the rate of reduction reduces (to 10-20%). This trend matches the conclusion of a similar study conducted for a conventional SPM machine [27].

The trend of normalized AC winding losses with the number of parallel strands/turn can also be analytically calculated using (5). The calculation assumes the magnetic field distribution to be unaffected across different parallel strands/turn and they are perpendicular to the strand width. Both the analytical and 2D FE results match well, as shown in Fig. 22(a).

The variation of AC winding loss against the number of parallel strands/turn with only armature currents excited is shown Fig. 22(b). For high slot/pole numbers, increasing the parallel strands/turn is not effective as the dominant source of losses is the armature slot leakage fluxes, the direction of which is almost parallel to the strand width. However, at lower slot/pole numbers, the armature fringing flux increases and therefore increasing parallel strands/turn becomes effective in reducing the AC winding losses. Again, increasing the parallel strands/turn from 1 to 2 is found to be most effective. With 4 parallel strands/turn, the losses could

be reduced by 57% and 23% for $P_r = 160$ and $P_r = 200$ compared to 1 strand/turn, respectively.

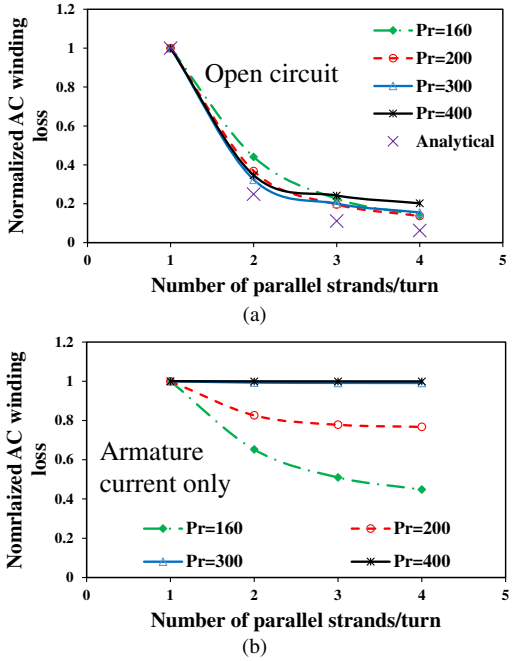


Fig. 22 Variations of AC winding loss against increasing number of parallel strands/turn for SPM-V machines with different slot/pole numbers. (a) Open-circuit. (b) Armature currents only conditions.

Although the circulating current losses are negligible compared to the AC winding losses, it would be interesting to know their trend with increasing number of parallel strands/turn. As shown in Fig. 23, it is observed that the circulating current losses show an increasing trend with the number of parallel strands/turn. This rate of increase is higher towards lower slot/pole numbers. The circulating current losses for the SPM-V machine with $P_r = 160$ and 4 parallel strands/turn can be almost 3.6 times (4.2 kW) higher than that compared to 2 strand/turn. A very similar trend of circulating current loss is observed with only armature current excited. A maximum circulating current loss of 1 kW is observed for the SPM-V machine with $P_r = 160$ and 4 parallel strands/turn. Although the circulating current losses are found to be significantly increasing with the number of parallel strands/turn, the absolute magnitudes are still negligible compared to the total AC winding loss.

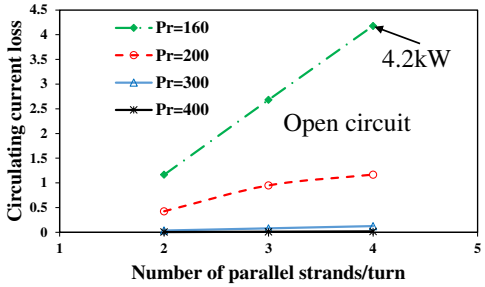


Fig. 23 Variations of open-circuit circulating current loss against increasing number of parallel strands/turn for the SPM-V machines with different slot/pole numbers.

### C. *Effects of Extra Clearance in Slot Opening*

The study of winding losses reveals that the majority of the losses are concentrated in the top conductors near the stator slot opening. Hence, it would be beneficial to provide extra clearance ($h_{ext}$) besides the top clearance (10 mm for wedge) as shown in Fig. 24. However, it is to be noted that the slot depth ($h_s$) remains unchanged. This would mean that the strand thickness reduces and therefore, assuming a constant rated current, the DC winding losses will increase. However, thinner conductors would also help to reduce the AC winding losses. Therefore, a tradeoff between the AC losses and DC losses could be achieved.

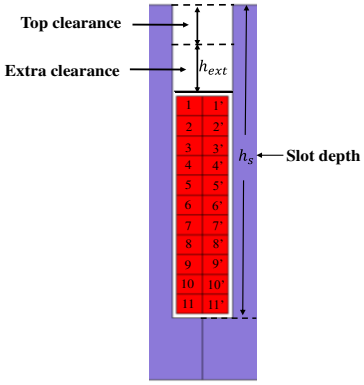


Fig. 24 Schematic showing the extra clearance ($h_{ext}$) in the slot opening.

To normalize the magnitude of the extra clearance for different slot/pole numbers, $\Delta h_{ext}$ is represented as a percentage of $h_s$ given by

$$\Delta h_{ext} = \frac{h_{ext}}{h_s} \times 100 \tag{7}$$

The variations of the total winding loss (including the DC loss) against $\Delta h_{ext}$ for SPM-V machines with different slot/pole numbers under rated load are shown in Fig. 25. The total winding losses are represented as a normalized value with the losses at $h_{ext} = 0$ for each slot/pole number being used as reference. It can be observed that for low slot/pole numbers, a small increase in the extra clearance shows a significant reduction in the total winding loss. This is mainly because of the reduced fringing flux linkage within the top strands. The comparison of the flux distribution in the slot at $\Delta h_{ext} = 0$ and $\Delta h_{ext} = 15$ for the SPM-V machine with $P_r = 160$ is shown in Fig. 26. This clearly shows the reduced fringing flux linking the top strands due to the extra clearance. At $\Delta h_{ext} = 15$, the total winding loss could be reduced by 55% for the SPM-V machine with $P_r = 160$. Beyond $\Delta h_{ext} = 15$, the clearance is less effective in reducing the winding losses as the rate of increase in DC loss is more significant than the rate of decrease in AC loss, as shown in Fig. 27(a). However, for high slot/pole numbers, the winding losses decrease linearly with an increase in $\Delta h_{ext}$, as shown in Fig. 27(b). This is largely due to the reduced strand thickness which is effective in reducing the losses due to the dominant slot leakage fluxes. Due to relatively higher AC winding losses than DC losses, the clearance is found to be effective across a wider range of $\Delta h_{ext}$. At $\Delta h_{ext} = 15$, the total winding losses could be reduced by 36% for the SPM-V machine with $P_r = 400$.

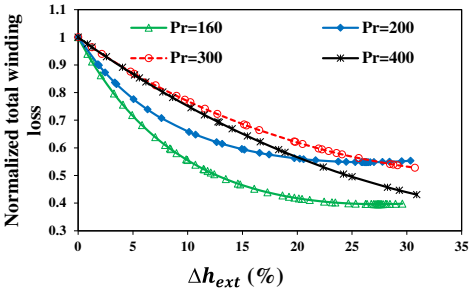


Fig. 25 Variations of total stator winding losses (including DC loss) against $\Delta h_{ext}$ under rated load condition.

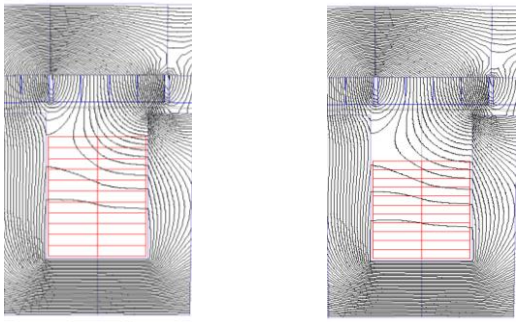

(a) (b)

Fig. 26 Comparison of flux distributions in the slot in SPM-V machine with $P_r = 160$. (a) $\Delta h_{ext} = 0$. (b) $\Delta h_{ext} = 15$.

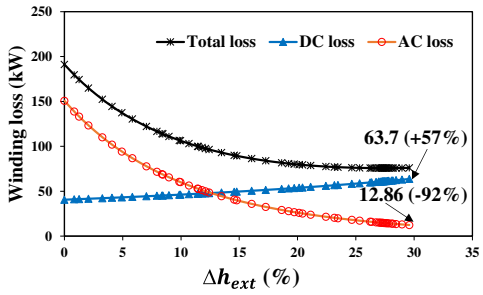


(a)

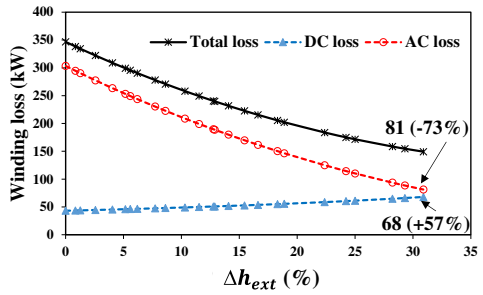


(b)

Fig. 27 Variations of AC and DC winding losses against $\Delta h_{ext}$ for the SPM-V machines with (a) $P_r = 160$ and (b) $P_r = 400$.

## VI. Effect of Proposed Flux Shunt Concept

This section proposes a novel flux shunt concept to reduce the AC winding losses in the SPM-V machines. The flux shunt is located near the slot opening (every slot) as shown in Fig. 28.

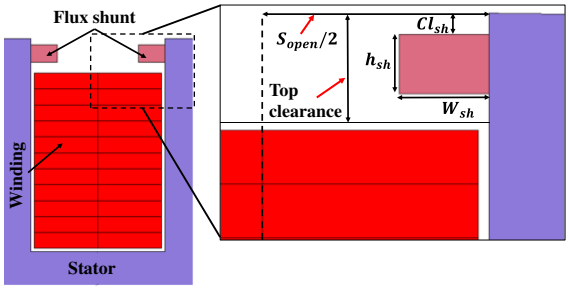


Fig. 28 Slot layout with the proposed flux shunt with relevant dimensions.

The flux shunt investigated in this paper has the same material and lamination direction as the stator iron core. Hence, the flux shunt is very similar to the tooth tips in conventional SPM machines with semi-close slots. However, for large machines, the semi-closed slot makes it difficult to install form-wound coils with large conductors. Hence, a separate flux shunt is proposed in this paper. One of the possible assemblies of the flux shunt is shown in Fig. 29(b). The proposed flux shunt can be integrated into the non-magnetic wedge and then inserted into a semi circular groove in the stator tooth from one side of the stator core. The existing conventional assembly with a non-magnetic wedge is shown in Fig. 29(a).

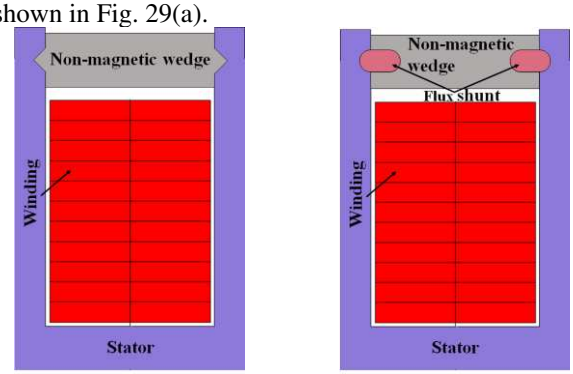


(a) (b)

Fig. 29 Schematic of slot layout. (a) With conventional non-magnetic wedge. (b) With flux shunt integrated into the non-magnetic wedge.

The main objective of the flux shunt is to bypass the fringing fluxes, linking with the conductors near the slot opening, through the flux shunt and thus reduce the AC winding losses. From the previous analyses, it is found that the fringing fluxes are the main source of AC winding losses of the SPM-V machines with lower slot/pole numbers. Hence the flux shunt concept is intended to reduce the AC winding losses towards lower slot/pole numbers where the SPM-V machines exhibit high torque capability. The positions and dimensions of the flux shunt for each slot/pole number are optimized using the variables highlighted in Fig. 28. The optimization is performed to achieve maximum torque and minimum AC winding losses. The analysis is carried out in the baseline design with 11 turns and 2 parallel strands per coil as presented in TABLE II.

### A. AC Winding Losses

The comparison of the AC winding losses (due to the 'rotor induced and proximity effect' component only) under rated load between different slot/pole number combinations of the SPM-V machines with and without flux shunt is shown in Fig. 30(a).

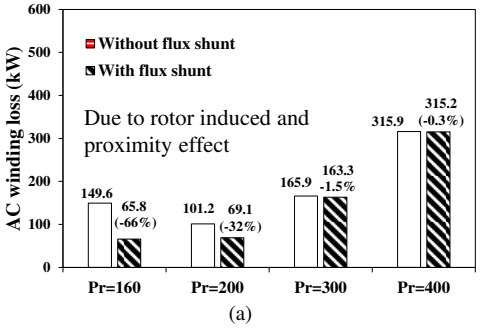


(a)

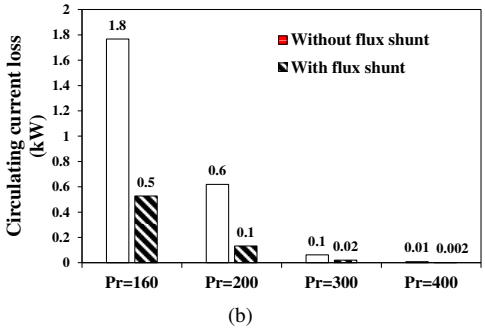


(b)

Fig. 30 Comparison of AC winding losses under rated load condition for different slot/pole number combinations of the SPM-V machines with and without flux shunt. (a) Loss due to 'rotor induced and proximity effect'. (b) Loss due to circulating current.

It is observed that the flux shunt is very effective in reducing the losses towards lower slot/pole numbers with almost 66% and 32% reduction for $P_r = 160$ and $P_r = 200$, respectively. However, as expected, the flux shunt has negligible impact on AC losses for high slot/pole numbers. Although the magnitude of circulating current losses is negligible in the investigated machines, the flux shunt is found to be very effective in reducing these losses, as shown in Fig. 30(b). The comparison of flux distribution under rated load condition for the SPM-V machine with $P_r = 160$ and with and without flux shunt is shown in Fig. 31. The bypassing of the fringing flux through the flux shunt can be easily observed in Fig. 31(b).

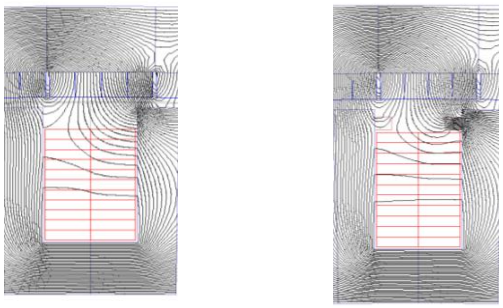

(a) (b)

Fig. 31 Comparison of flux distributions in the slot in SPM-V machine with $P_r = 160$. (a) Without flux shunt. (b) With flux shunt.

## B. Torque and Power Factor

The flux shunt near the slot opening can alter the airgap permeance and may affect the torque. The comparison of open circuit radial airgap flux density and their spectra, with and without flux shunt, for the SPM-V machine with $P_r = 160$ is shown in Fig. 32.

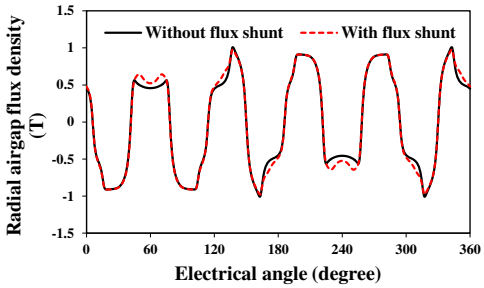


(a)

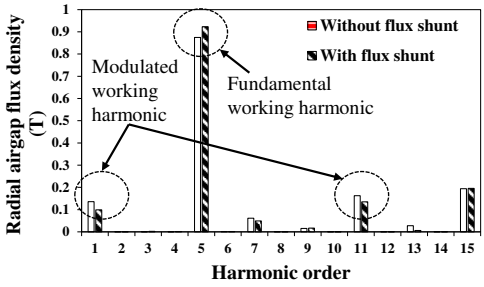


(b)

Fig. 32 Comparison of open-circuit radial airgap flux densities with and without flux shunt for an SPM-V machine with $P_r = 160$. (a) Waveform and (b) Spectra.

The comparison of average torque with and without flux shunt, for different slot/pole numbers of the SPM-V machines, is shown in Fig. 33. The torque is found to be reduced by 3.7% and 3% for $P_r = 160$ and $P_r = 200$, respectively. These reductions in torque are marginal compared to the benefits achieved in AC winding loss reduction. It is interesting to note that the toque slightly increases for $P_r = 400$. This is due to the aforementioned increase in the fundamental airgap flux density. At high slot/pole numbers, this fundamental component dominates the average torque contribution compared to the modulated ones.

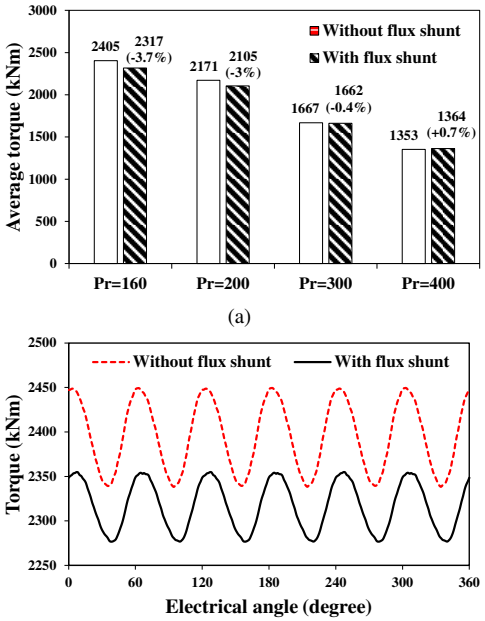


(a)




(b)

Fig. 33 Comparison of torque of SPM-V machines with and without flux shunt. (a) Average torque for different slot/pole numbers. (b) Torque waveforms for $P_r = 160$.

TABLE IV. PERFORMANCE COMPARISON WITH AND WITHOUT FLUX SHUNT FOR DIFFERENT SLOT/POLE NUMBERS OF THE SPM-V MACHINES

| Rotor pole pair | Presence of flux shunt | Torque ripple (%) | Cogging torque (%) | Power factor |
|---|---|---|---|---|
| 160 | Without shunt | 4.63 | 3.21 | 0.49 |
| | With shunt | 3.37 | 3.7 | 0.44 |
| 200 | Without shunt | 3.62 | 0.71 | 0.45 |
| | With shunt | 2.67 | 2.1 | 0.41 |
| 300 | Without shunt | 1.76 | 1.46 | 0.39 |
| | With shunt | 2.38 | 2.19 | 0.37 |
| 400 | Without shunt | 0.82 | 0.66 | 0.32 |
| | With shunt | 0.97 | 0.68 | 0.3 |

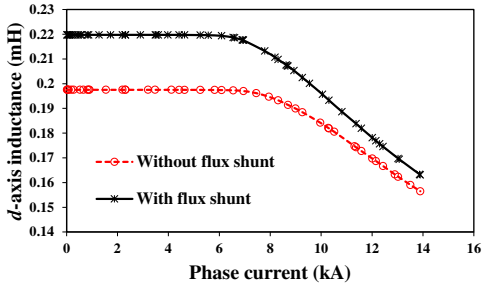


Fig. 34 Comparison of $d$-axis inductance with and without flux shunt for the SPM-V machine with $P_r = 160$.

As an example, the comparison of torque waveforms of the SPM-V machines with $P_r = 160$ and with and without flux shunt is shown in Fig. 33(b). It can be observed that the torque ripple is reduced by using the flux shunt. The comparison of torque ripple, cogging torque and power factor, with and without flux shunt, for different slot/pole numbers of the SPM-V machines, is shown in TABLE IV. Because of increased PM flux due to the introduced flux shunt, the cogging torque is found to increase. However, for lower slot/pole numbers, the flux shunt helps reduce the saturation and thereby the overall torque ripple. It also reduces the power factor by around 10%. This is mainly due

to the fact that the flux shunt is found to increase the synchronous inductance, as shown in Fig. 34. Here, the SPM-V machine with $P_r = 160$ is selected as an example.

### C. Efficiency

The impact of flux shunt on the overall efficiency of the SPM-V machines is shown in Fig. 35(a). The significant reduction in AC winding losses has helped to improve the efficiency by 1.8% and 0.6% for $P_r = 160$ and $P_r = 200$, respectively. However, although the introduction of flux shunt does not affect the PM eddy current losses, the iron core losses are found to be increased by 8-12%, as shown in Fig. 35(b).

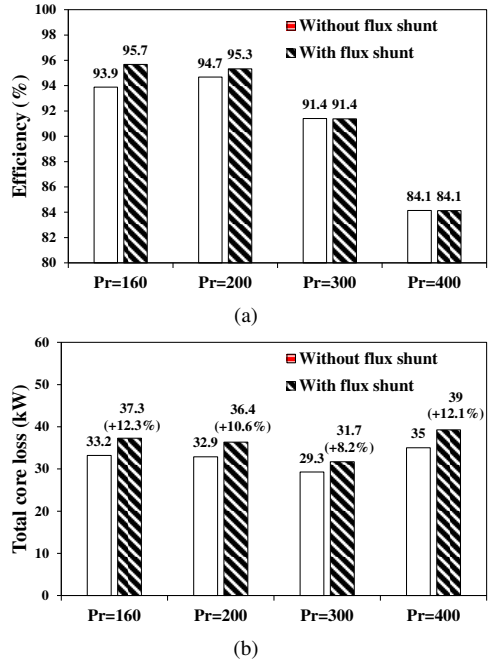


Fig. 35 Comparison of efficiency and iron core loss for different slot/pole numbers of the SPM-V machines with and without flux shunt. (a) Efficiency. (b) Iron core loss (including stator and rotor cores and flux shunt iron losses).

The increase in iron core loss is largely contributed by the stator iron core loss due to the higher penetration of PM flux. Whereas the losses in the flux shunt itself and its impact on rotor iron core losses are found to be negligible.

### D. Demagnetization

It has been revealed that irreversible demagnetization is a critical problem for SPM-V machines for high power ratings, especially towards lower slot/pole numbers [30]. Hence, it would be important to investigate the impact of flux shunt on the demagnetization performance. The analysis is carried out for a 3-phase symmetrical short circuit condition and the approach adopted in this paper is the same as that presented in [30].

The risk of irreversible demagnetization is high for SPM-V machines with low slot/pole number because of their high phase inductance. Hence, as an example, the SPM-V machine with $P_r = 160$ has been chosen to show the effect of flux shunt on demagnetization performance. The comparison of the $d$-axis current with and without flux shunt is shown in Fig. 36. The peak value of $d$-axis current ($I_{d,peak}$) is marginally reduced by 6.5% with the flux shunt due to their higher synchronous inductance. The flux density distribution in the magnet and the flux distribution in the machine at $I_{d,peak}$ are compared for machines with and without flux shunt, as shown in Fig. 37. Here the rotor position is at $d$-axis where maximum demagnetization occurs. The flux density below the knee point (0.12 T), where the demagnetization occurs, is shown using a coloured map. It can be observed that the flux shunt helps to alleviate the risk of irreversible demagnetization in the SPM-V machines.

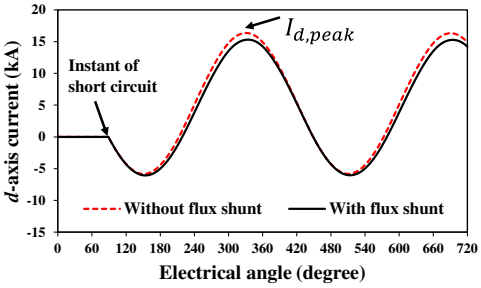


Fig. 36 Comparison of $d$-axis current under 3-phase short circuit with and without flux shunt for the SPM-V machine with $P_r = 160$.

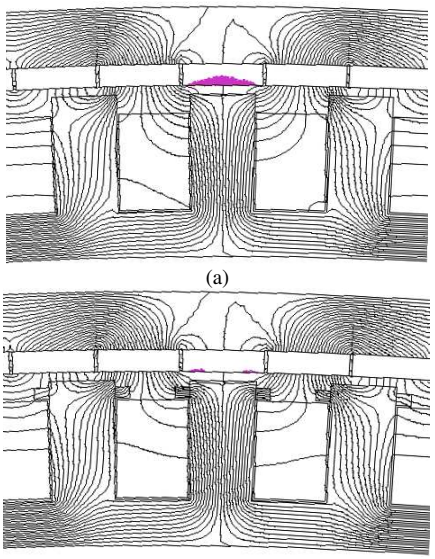


Fig. 37 Comparison of $d$-axis flux distribution in the machine and the flux density distribution in the magnet at $I_{d,peak}$ for the SPM-V machine with $P_r = 160$. (a)Without flux shunt. (b) With flux shunt. The coloured region in the magnet indicates the demagnetized region.

In summary, the above study reveals that the effectiveness of a particular loss reduction technique depends on the slot/pole number combinations for the SPM-V machines. The AC losses characteristics would also vary according to the operating conditions and the type of windings used. Hence, the loss reduction techniques discussed above should be carefully selected and optimized according to the specific applications. The following major deductions can be made from the above study:

- For designs with high slot leakage fluxes (usually for high slot/pole numbers), it is better to use thinner conductors by either increasing the number of turns/coil or by providing extra clearance. Increasing the number of parallel strands/turn and a flux shunt may not be effective.
- For designs with high fringing fluxes (usually for low slot/pole numbers), it is better to apply techniques like increasing the parallel strands/turn, using a flux shunt and providing extra clearance that can effectively reduce the losses in the top conductors near the slot opening.

## VII. Loss Comparison For Final Design

For the final performance comparison, the SPM-V machines with 22 turns/coil and 4 parallel strands/turn have been selected. The number of turns/phase for the SPM-V machines has been kept constant as 22, which is similar to the baseline design discussed in TABLE II. The maximum value of extra clearance ($h_{ext}$) that can be used is also limited by the minimum strand thickness (2 mm) considering the practical manufacturing challenges. Therefore, the extra clearance has been chosen as 15%, beyond which the strand thickness is below 2 mm for $P_r = 160$, as shown in Fig. 38. The flux shunt has been used only for the lower slot/pole number SPM-V machines, i.e. $P_r = 160$ and $P_r = 200$, as they have limited effect on AC winding loss reduction for high slot/pole numbers.

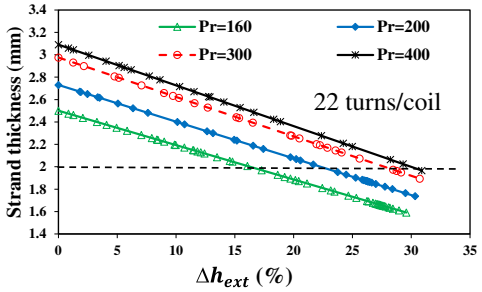


Fig. 38 Reduction of strand thickness with increasing $\Delta h_{ext}$ for different slot/pole numbers of SPM-V machines.

The final stator winding losses for the SPM-V machines with different slot/pole number combinations in comparison with the conventional SPM machines under rated load condition are shown in Fig. 39.

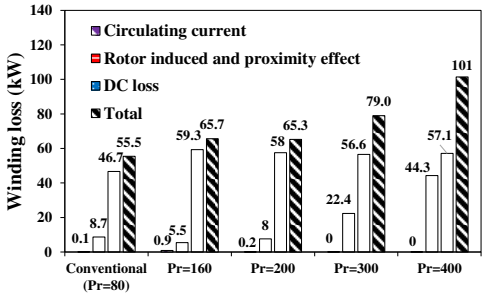


Fig. 39 Comparison of final winding losses under rated condition between conventional SPM and SPM-V machines with different slot/pole numbers.

It can be observed that the loss reduction techniques are very effective in reducing the AC winding losses of the SPM-V machines. The minimum value of the AC winding loss achieved by the SPM-V machines with $P_r = 160$ is 5.5 kW (reduced by 96.3% from 149.6 kW), which is lower than that (8.7 kW) of the conventional SPM machine. For the highest slot/pole number combination ($P_r = 400$), the AC winding loss was reduced by 86% from 315.9 kW to 44.3 kW.The electromagnetic losses after implementing the loss reduction techniques are compared in Fig. 40(a). The minimum value of total loss (112.6 kW) for the SPM-V machine is achieved for $P_r = 200$, which is still 34% higher than that (83.8 kW) of the conventional SPM machine. However, due to the higher torque produced by the SPM-V machine, the optimal efficiency achieved (96.9%) at $P_r = 160$ is comparable to that of the conventional SPM machine, as shown in Fig. 40(b). It is worth noting that although the SPM-V machines with lower slot/pole numbers are emerging as a better choice in terms of efficiency, they may still have higher copper loss/surface area (slot wall area) that brings forth cooling challenges. Similarly, the impact of high PM eddy loss towards lower pole numbers would also need careful investigation.

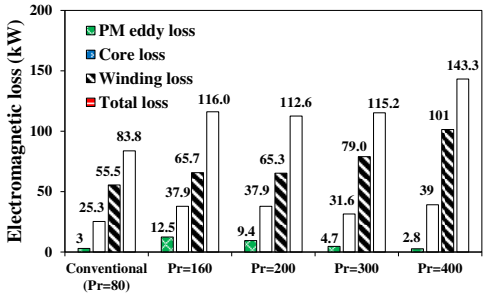


(a)

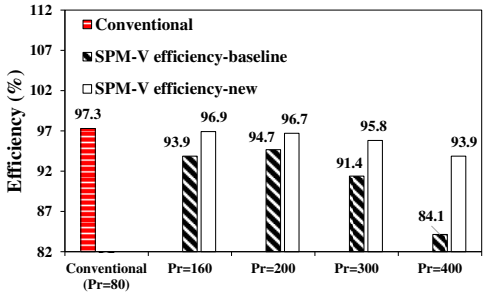


(b)

Fig. 40 Comparison of electromagnetic losses and efficiency. (a) Electromagnetic losses. (b) Efficiency between the conventional SPM and SPM-V machines with different slot/pole number combinations. 'Efficiency-baseline' refers to the efficiency of the SPM-V machines designs with 11 turns and 2 parallel strands/turn. 'Efficiency-new' refers to efficiency after implementing the loss reduction techniques.

## VIII. Conclusion

The AC winding losses for the 3 MW SPM-V machines with different slot/pole number combinations have been investigated. The losses have been benchmarked against a conventional SPM machine. The study shows that the total AC winding losses for the SPM-V machines, especially towards high slot/pole numbers (315.9 kW), are significantly higher than the conventional SPM machines (8.7 kW). This is mainly due to their high operating frequencies at high slot/pole numbers. Whereas, at low slot/pole numbers, the AC winding losses (149.6 kW) are driven by high PM and armature fringing fluxes due to their large slot openings. A novel flux shunt concept has been proposed to reduce the AC winding losses in the SPM-V machines, which is found to be very effective towards lower slot/pole numbers. Moreover, the effectiveness of other conventional AC winding loss reduction techniques such as increasing the number of turns/coil and parallel strands/turn, providing extra clearance in slot opening have also been studied. It is found that by implementing these techniques, the efficiencies of the SPM-V machines can be significantly improved and can be comparable to that of the conventional SPM machines. Moreover, the proposed flux shunt concept has the potential to reduce the risk of irreversible demagnetization in the SPM-V machines.

## References

[1] G. van de Kaa, M. van Ek, L. M. Kamp, and J. Rezaei, "Wind turbine technology battles: Gearbox versus direct drive - opening up the black box of technology characteristics," *Technological Forecasting and Social Change*, vol. 153, p. 119933, 2020.

[2] T. M. Jahns, "The expanding role of PM machines in direct-drive applications," in *Proc. Int. Conf. Elect. Mach. Syst. (ICEMS)*, Beijing, China, Aug. 2011, pp. 1–6.

[3] S. Alshibani, V. G. Agelidis, and R. Dutta, "Lifetime cost assessment of permanent magnet synchronous generators for MW level wind turbines," *IEEE Trans. Sustain. Energy*, vol. 5, no. 1, pp. 10–17, Jan. 2014.

[4] P. M. Tlali, R.- Wang, and S. Gerber, "Comparison of PM Vernier and conventional synchronous 15 kW wind generators," in *Proc. 13th Int. Conf. Elect. Mach.*, Alexandroupoli, Greece, 2018, pp. 2065–2071.

[5] D. K. Kana Padinharu, G. J. Li, Z. Q. Zhu, R. Clark, A. S. Thomas, and Z. Azar, "System-level investigation of multi-MW direct-drive wind power PM Vernier generators," *IEEE Access*, vol. 8, pp. 191433–191446, 2020.

[6] J. Li, K. T. Chau, J. Z. Jiang, C. Liu, and W. Li, "A new efficient permanent-magnet vernier machine for wind power generation," *IEEE Trans. Magn.*, vol. 46, no. 6, pp. 1475–1478, Jun. 2010.

[7] I. Mény, P. Enrici, J. J. Huselstein, and D. Matt, "Wind power system for domestic installations," *ICREPQ'04*, vol. 1, 2004.

[8] K. Xie, D. Li, R. Qu, X. Ren, M. R. Shah, and Y. Pan, "A new perspective on the PM Vernier machine mechanism," *IEEE Trans. Ind. Appl.*, vol. 55, no. 2, pp. 1420–1429, 2019.

[9] D. K. Kana Padinharu, G. J. Li, Z. Q. Zhu, R. Clark, Z. Azar, and A. Thomas, "Investigation of scaling effect on power factor of permanent magnet Vernier machines for wind power application," *IET Electric Power Applications*, vol. 14, no. 11, pp. 2136–2145, Jul. 2020.

[10] Y. Liu, H. Y. Li, and Z. Q. Zhu, "A high-power factor Vernier machine with coil pitch of two slot pitches," *IEEE Trans. Magn.*, vol. 54, no. 11, pp. 1–5, Nov. 2018.

[11] L. Wu, R. Qu, D. Li, and Y. Gao, "Influence of pole ratio and winding pole numbers on performance and optimal design parameters of surface permanent-magnet Vernier machines," *IEEE Trans. Ind. Appl.*, vol. 51, no. 5, pp. 3707–3715, Sep. 2015.

[12] S. Hyoseok, N. Niguchi, and K. Hirata, "Characteristic analysis of surface permanent-magnet Vernier motor according to pole ratio and winding pole number," *IEEE Trans. Magn.*, vol. 53, no. 11, Nov. 2017.

[13] Y. Gao, R. Qu, J. Li, Z. Zhu, and D. Li, "HTS vernier machine for direct-drive wind power generation," *IEEE Trans. Appl. Supercond.*, vol. 24, no. 5, Oct. 2014.

[14] D. A. Gonzalez and D. M. Saban, "Study of the copper losses in a high-speed permanent-magnet machine with form-wound windings," *IEEE Trans. Ind. Electron.*, vol. 61, no. 6, pp. 3038–3045, 2014.

[15] N. Taran, V. Rallabandi, D. M. Ionel, G. Heins, and D. Patterson, "A comparative study of methods for calculating AC winding losses in permanent magnet machines," in *Proc. IEEE Int. Elect. Mach. Drives Conf. (IEMDC)*, 2019, pp. 2265–2271.

[16] F. Jiancheng, L. Xiquan, B. Han, and K. Wang, "Analysis of circulating current loss for high-speed permanent magnet motor," *IEEE Trans. Magn.*, vol. 51, no. 1, pp. 1–13, 2015.

[17] P. Ponomarev, I. Petrov, N. Bianchi, and J. Pyrhönen, "Additional losses in stator slot windings of permanent magnet synchronous machines," *Electronic Open-Access Publication*, May 2015.

[18] A. S. Thomas, Z. Q. Zhu, and G. W. Jewell, "Proximity loss study in high speed flux-switching permanent magnet machine," *IEEE Trans. Magn.*, vol. 45, no. 10, pp. 4748–4751, 2009.

[19] A. Al-Timimy, P. Giangrande, M. Degano, M. Galea, and C. Gerada, "Investigation of AC copper and iron losses in high-speed high-power density PMSM," in *Proc. 13th Int. Conf. Elect. Mach*, Alexandroupoli, Greece, 2018, pp. 263–269.

[20] S. Iwasaki, R. Deodhar, Y. Liu, A. Pride, Z. Q. Zhu, and J. Bremner, "Influence of PWM on the proximity loss in permanent magnet brushless AC machines," in *IEEE Ind. Appl. Soc. Ann. Meeting*, Edmonton, Alberta, Canada, Oct. 2008, pp. 1–8.

[21] G. J. Atkinson, B. C. Mecrow, A. G. Jack, D. J. Atkinson, P. Sangha, and M. Benarous, "The analysis of losses in high-power fault-tolerant machines for aerospace applications," *IEEE Trans. Ind. Appl.*, vol. 42, no. 5, pp. 1162–1170, 2006.

[22] M. van der Geest, H. Polinder, J. A. Ferreira, and D. Zeilstra, "Stator winding proximity loss reduction techniques in high speed electrical machines," in *Proc. Int. Elect. Mach. Drives Conf*, 2013, pp. 340–346.

[23] M. J. Islam and A. Arkkio, "Effects of pulse-width-modulated supply voltage on eddy currents in the form-wound stator winding of a cage induction motor," *IET Electric Power Applications*, vol. 3, no. 1, pp. 50-58(8), Jan. 2009.

[24] C. Yicheng, P. Pillay, and A. Khan, "PM wind generator topologies," *IEEE Trans. Ind. Appl.*, vol. 41, no. 6, pp. 1619–1626, 2005.

[25] D. K. Kana Padinharu, G. J. Li, Z. Q. Zhu, M. P. Foster, D. A. Stone, A. Griffo, R. Clark, and A. Thomas, "Scaling effect on electromagnetic performance of surface mounted permanent magnet Vernier machine," *IEEE Trans. Magn.*, vol. 56, no. 5, pp. 1–15, May 2020.

[26] T. A. Lipo, "Use of magnetic circuits in leakage reactance calculations," in *Introduction to AC Machine Design*, John Wiley & Sons, Ltd, 2017, pp. 125–191.

[27] L. J. Wu and Z. Q. Zhu, "Simplified analytical model and investigation of open-circuit AC winding loss of permanent-magnet machines," *IEEE Trans. Ind. Electron.*, vol. 61, no. 9, pp. 4990–4999, 2014.

[28] W. Huang, A. Bettayeb, R. Kaczmarek, and J. Vannier, "Optimization of magnet segmentation for reduction of eddy-current losses in permanent magnet synchronous machine," *IEEE Trans. Energy Convers*, vol. 25, no. 2, pp. 381–387, 2010.

[29] L. Wu and Z. P. Xia, "Stator tooth segmentation method for electric machines," EP2757662A1.

[30] D. K. Kana Padinharu, G. J. Li, Z. Q. Zhu, M. P. Foster, D. A. Stone, A. Griffo, M. Odavic, R. Clark, and A. Thomas, "Influence of demagnetization on selecting the optimum slot/pole number combination for 3MW surface mounted permanent magnet Vernier machine," in *Proc. 22nd Int. Conf. Electr. Mach. Syst. (ICEMS)*, Harbin, China, Aug. 2019, pp. 1–6.